Overtopping hazard on a rubble mound breakwater

Ana R. Carrasco†, Maria T. Reis††, Maria G. Neves††, Óscar Ferreira†, Ana Matias†, Sílvia Almeida†

†CIMA, Universidade do Algarve,
Campus de Gambelas
8005-139, Faro, Portugal
azarcos@ualg.pt
oferreir@ualg.pt
ammatias@ualg.pt
smalmeida@ualg.pt

††LNEC – National Laboratory for Civil
Engineering
Av. do Brasil, 101
1700-066 Lisboa, Portugal
treis@lnec.pt
gneves@lnec.pt

www.cerf-jcr.org

www.JCRonline.org

ABSTRACT

Carrasco, A.R., Reis, M.T., Neves, M.G., Ferreira, Ó., Matias, A, Almeida, S., 2014. Overtopping hazard on a rubble mound breakwater. *In:* Green, A.N. and Cooper, J.A.G. (eds.), *Proceedings 13th International Coastal Symposium* (Durban, South Africa), *Journal of Coastal Research*, Special Issue No. 70, pp. 247-252, ISSN 0749-0208.

A major concern of coastal engineering is not only to access the damage to coastal structures by severe wave overtopping, but also the hazard imposed to users. Local hazard is often associated to the volume of overtopping water per unit of time (called overtopping discharge). Despite two decades of intensive research, it is yet not fully clear to practitioners what is the best method to compute the discharge parameter and its application on the assessment of local hazard. This work provides insight into the overtopping characterization in rubble mound breakwaters, by distinguishing different methods to assess hazardous overtopping. Fieldwork was conducted over a tidal cycle in a breakwater located at Albufeira Harbour (South coast of Portugal) under storm conditions (Hso~ 3 m; Tp ~ 9 s). Mean overtopping discharges were calculated from field measurements of flow depths and velocities at the breakwater slope armour and at the impermeable crest. Two different velocities were calculated: overtopping leading-edge velocity and overtopping peak velocity. The two methods provided similar results, with higher velocities occurring during high-tide (between 2 and 10 m/s). Mean overtopping discharges at the beginning of the impermeable crest ranged between 0.2 and 0.8 l/s/m. Under the measured hydrodynamic conditions, the breakwater offers risk to all types of pedestrians.
Additionally it is shown that field measurements compare relatively well with empirical prediction methods (for the overall analysed overtopping events), namely the corrected NN_OVERTOPPING2 neural network tool. Besides contributing to the overall database on wave overtopping in coastal structures, the presented results can also be used for calibration and validation of overtopping evaluation methods (empirical formulae, artificial neural networks and numerical and physical models).

ADDITIONAL INDEX WORDS: *wave, discharge, velocities, hazard, empirical prediction.*

INTRODUCTION

Most sea defence structures are constructed primarily to limit overtopping volumes that might cause flooding (Shankar and Jayaratne, 2003). Flooding potential is determined from the quantity of overtopping water per unit of time (overtopping discharge) and storm duration (Chini and Stansby, 2012; Hughes *et al.*, 2012; Tonelli and Petti, 2013). Over a storm or tide, the overtopping volumes that can be tolerated will be site specific, as the volume of water that can be permitted will depend on the size and use of the receiving area, extent and magnitude of drainage ditches, damage versus inundation curves, and return period (Pullen *et al.*, 2007). Ideally, return periods at which overtopping hazards are analysed, and against which a defence might be designed, should be constantly set by national regulation or guidelines, yet that is not common practice (Geeraerts *et al.*, 2007).

The main hazards on or close to sea defence structures are of death, injury, property damage or disruption from direct wave impact or by drowning (Geeraerts *et al.*, 2007). Some guidance has been given on the basis of the tolerable discharges and overtopping volumes for a range of circumstances or uses (Pullen

et al., 2007; Geeraerts *et al.,* 2007), which have been widely used in several locations. The EurOtop Manual gives guidance on allowable overtopping when people are present or vehicles are moving behind the structure.

Hazard-driven flow parameters are essentially the mean overtopping discharge and the maximum overtopping volume, as well as overtopping flow depths and velocities. The mean overtopping discharge is the most widely used to judge allowable overtopping. An extensive database on mean overtopping discharge has been gathered in the scope of the CLASH project (http//:www.clash-eu.org). However, the mean discharge does not always describe the real behaviour of wave overtopping, where only the larger incoming waves will reach the top of the structure and promote overtopping. There remain also two difficulties in specifying safety levels with reference to maximum volumes rather than to mean discharges. Firstly, methods to predict maximum volumes are available for limited structure types, and are not well-validated. Secondly, data relating individual maximum overtopping volumes to hazard levels are still very rare (Pullen *et al.*, 2007).

The ideal situation is to instrumentally collect data at each required location and locally define the hazard thresholds. That is however a very remote possibility for the vast majority of the existing structures. Even if it is possible to collect data, often there is no constant discharge over the crest of a structure. That is the

case when accessing very thin water layers of run-up tongues, which are common in rubble mound revetments, because they are porous and have sloping layers, dissipating a large proportion of the incident wave energy (Pullen *et al.*, 2007). In fact, few investigations have been conducted on rough slopes of different sizes of armour (Shankar and Jayaratne, 2003). Hazard driving flow parameters are nowadays recurrently predicted based on engineering models and formulae resulting from recent experiments. Indeed, in the past two decades, wave overtopping was investigated in a large number of studies and projects, mostly of experimental nature (e.g. De Rouck *et al.*, 2005; Van der Meer *et al.*, 2006), which led to the development of several empirical prediction formulae and artificial neural networks (Verhaeghe, 2005; Pullen *et al.*, 2007). Notwithstanding, the overtopping results obtained from the derived models still have a large degree of uncertainty, as the models themselves demand a continued calibration. The present work uses a dataset of collected overtopping flow depths and velocities in a rubble mound breakwater in Portugal with two aims: (a) full characterization of overtopping conditions based on fieldwork data, and (b) their comparison with mean discharges predicted by empirical tools.

METHODS

Experimental setting

Overtopping experiments were conducted at the west breakwater of Albufeira Harbour (South coast of Portugal, Figure 1) on the 19th January 2013 from 4 am till 12 pm. The chosen breakwater is a relatively low-crested structure (4.3 m above mean sea level, MSL) with about 42 % porosity (Eric Didier, personal communication). It is of easy access and it is often overtopped by waves higher than 3 m during spring tides. In the fishing harbour protected by the breakwater, small fishing boats are anchored more than 20 m from the rear slope of the structure. Details about the structure can be found in Didier *et al.* (2011). The collected and analysed data included tidal levels, wave characteristics (offshore and at the structure), and overtopping parameters (flow depth, velocity and associated discharge). For the analysis of the overtopping variability, the monitored tidal cycle was divided in several blocks of 30 minutes.

Nearshore and offshore measurements

Tidal data were obtained from Huelva tide gauge (Spain), located at about 100 km to the East of the study area. The recorded levels (referred to the local harbour level) were corrected for the Portuguese datum and mean sea level (MSL). A time correction (~30 minutes tide delay in Albufeira) was also performed. Offshore wave height (significant, Hso, and maximum, Hmaxo) and peak period (Tp) were obtained from Faro wave buoy (belonging to Instituto Hidrográfico), located 30 km to the East of the study area (Figure 1a) in a water depth of 93 m MSL. Overtopping parameters (flow depth and velocity) were measured along a profile in the middle section of the western breakwater (Figure 1b and c). Flow depth was measured with a series of pressure transducers along the breakwater crest. Video images from crest overtopping at the profile of instrumentation were recorded from a higher position at a nearby cliff (100 m in horizontal distance, Figure 1b). Ground Control Points (GCPs) were placed and georeferenced to support overtopping flow analysis using video image.

Nearshore wave propagation

Offshore wave conditions were propagated to the breakwater toe (3.5 m below MSL) using SWAN (Simulating WAves Near-shore; Booij *et al.*, 1999). Grid resolutions of 45 m and 5 m were chosen for the large and small grids, respectively (Figure 2).

Model predictions were initialized on the two open boundaries of the larger grid with the parametric input from the wave buoy time series, using a JONSWAP spectral shape to represent the wave field. Input boundary conditions for the small grid were determined from the computations over the large grid. SWAN simulations accounted for non-linear triad wave-wave interactions,
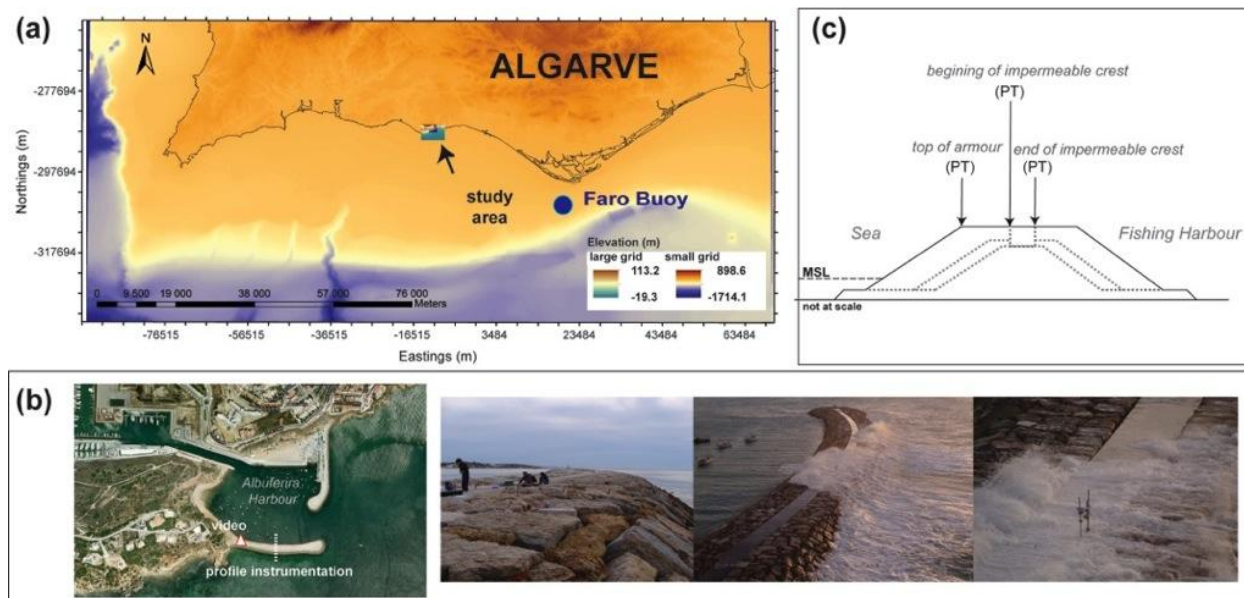

Figure 1. (a) Study area; (b) Albufeira Harbour and photos from fieldwork profile instrumentation and overtopping occurrence; and (c) Pressure transducers (PT) location across the breakwater profile.
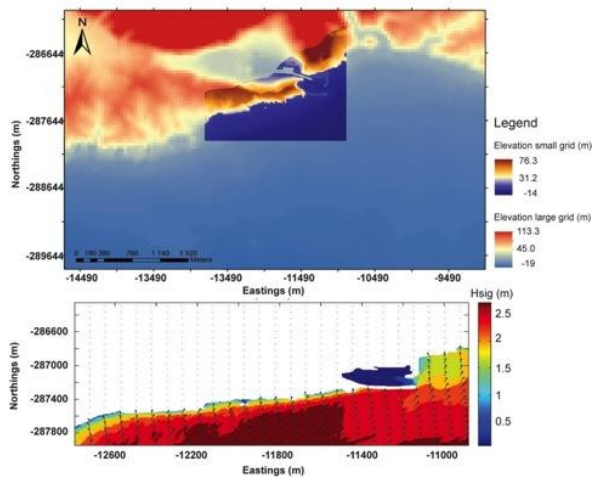
Figure 2. Nested grids used in SWAN runs (depths referred to MSL, upper panel). Significant wave height (Hs), and wave direction (arrows), during high tide (lower panel).

as they are rather important in shallow coastal areas (Booij *et al.*, 1999; Holthuijsen, 2007), for bottom friction dissipation using the default variable JONSWAP expression according to Hasselmann *et al.* (1973), and for breaking dissipation according to the default bore-based model of Battjes and Janssen (1978).

Overtopping velocities and discharge computations

Each overtopping event was defined as a single passage of water above the structure crest. Data were collected at the top of the armour slope and at the beginning of the impermeable crest of the breakwater (distant 5.2 m). These data were used to identify overtopping frequency, and to calculate flow depth and flow velocity.

The leading-edge flow velocity (v_f) represents the water velocity between the sensors located at the top of the armour slope and at the beginning of the impermeable crest, and is obtained using the time delay between sensors:

$$vf = \frac{d}{tf - ti} \qquad (1)$$

where *d* is the horizontal distance between the sensors, *ti* and *tf* correspond to the arrival time at the top of the slope armour and the arrival time at the beginning of the impermeable crest, respectively. The leading-edge velocity, v_f, represents the mean velocity of each event. Besides, peak overtopping flow velocity (v_p) was also computed by considering the difference between arrival times of maximum overtopping flow depths (peak):

$$vp = \frac{d}{tpf - tpi} \qquad (2)$$

where *tpi* and *tpf* correspond to the arrival times at the top of the armour and at the beginning of the impermeable crest, respectively. Overtopping leading-edge volumes (V_f) and overtopping peak volumes (V_{max}), were also calculated for all overtopping events, using the flow depths, flow velocities (leading-edge velocity and peak velocity) and the duration of each event.

Empirical tools prediction

Calculated mean overtopping discharges based on field measurements at the top of the armour (Qarmour) and at the beginning of the impermeable crest (Qcrest) were compared with mean discharges predicted by the EurOtop empirical formulae

available online (http://www.overtopping-manual.com/calculation_tool.html) and by the NN_OVERTOPPING2 tool (Coeveld *et al.*, 2005) also available online. For comparison, the calculated mean overtopping discharges for each block of 30 minutes (Qarmour and Qcrest), were obtained by adding all event volumes and dividing by 1800 s.

The geometrical characteristics of the structure adopted for the discharge prediction were defined according to six cross-sections measured around the instrumented profile. For the EurOtop formulae the structure geometry was assumed as "armoured composite slope with crest berm". The input wave parameters at the toe of the structure and the structure parameters are described in Ferreira *et al.* (2013). Input wave parameters for the NN_OVERTOPPING2 tool included the wave data at the toe of the structure and the angle between the wave direction and the normal to the structure. Details about the NN_OVERTOPPING2 input parameters are presented in Coeveld *et al.* (2005). For both methods, EurOtop formulae and NN_OVERTOPPING2, the predicted mean overtopping discharges are provided per meter run of seawall.

Hazard assessment

Hazard assessment was conducted by comparing calculated mean overtopping discharges and maximum volumes, both based on filed measurements, with the values indicated in the EurOtop Manual (2007) and Geeraerts *et al.* (2007). The overtopping limits suggested in Table 1 derivate from a general precautionary principle based on observations and measurements undertaken by the CLASH project (Allsop *et al.*, 2008). Above the presented limits, both humans and goods are at risk; risk to structure integrity is not evaluated here.

RESULTS AND DISCUSSION

Overtopping parameters (flow depths and flow velocities) were measured during neap tides and storm conditions (Hso ~ 3-4 m and Tp ~ 8-10 s, Figure 3), with dominant wave direction from SW, frequent during winter. Maximum wind intensities were close to 7 m/s, occurring during high tide. For the analysis of the overtopping variability along the monitored tidal cycle, four blocks of 30 minutes, beginning at 05h, 07h, 08h and 10h, were chosen; each time block represents different tide stages. The time block of 05h represents the beginning of overtopping occurrence, whereas the time blocks of 07h and 08h are representative of high tide, and the time block of 10h is representative of mid tide (Figure 3a).

Overtopping frequency and associated discharges

Overtopping flow was generally turbulent across the armour and the end of the impermeable crest of the breakwater, similar to 'white water' flow defined by Pullen *et al.* (2007). Indeed, most recorded flows are classified with mean Froude number of 9 (supercritical). The maximum overtopping duration was 5 s, and mean overtopping flow depths were on average below 3 cm (Figure 4). There is no significant correlation between the flow depths and related velocities, which means that the higher velocities were not always related with deeper water flows. Mean v_f and v_p values are of the same order of magnitude, less than 6 m/s; maximum values obtained for v_f are slightly higher than for v_p, due to differences in the methodology (Figure 4). Results for v_f were corroborated with velocities obtained with video analysis (using wave arrival at each GCPs). The velocities obtained with

Table 1. Indicated limits for overtopping mean discharges and peak volumes (adapted from Geeraerts *et al.*, 2007).

Hazard type/reason	Mean discharge	Peak volume
Pedestrians	Q (l/s/m)	Vmax (l/m)
Unaware pedestrian, no clear view of the sea, narrow walkway or close proximity to edge	Q > 0.03	2 – 5 at high level or velocity
Aware pedestrian, clear view of the sea, wider walkway	Q > 0.1	20 - 50 at high level or velocity
Trained staff, well shod and protected, overtopping flows at lower levels only, no falling jet, low danger of fall from walkway	Q [1 – 10]	500 at low level
Marinas		
Sinking of small boats set 5-10 m from wall, damage to larger yachts	Q > 10	1000-10000
Significant damage or sinking of larger yachts	Q > 50	5000-50000

video image were, on average 5 m/s, with maximum values of 12 m/s.

Larger overtopping volumes were recorded during high tide (07h and 08h, Table 2), as well as higher flow depths and higher velocities (Figure 4). The increased velocities might be partially ascribed to an increase in overtopping depth and also to an increase of wind velocity over that period. Wind affected incoming waves by blowing up-rushing water over the crest of the structure, resulting in a possible modification of the physical form of the overtopping volume or jet (Pullen *et al.*, 2007), and ultimately, contributing to the total volume of overtopping. Wind also affects the way that hazard might be assessed (Shankar and Jayaratne, 2003; Allsop *et al.,* 2008). Obtained records are, however, scarce to yield conclusions.

Except for 05h time block, mean V_{max} values are of higher magnitude than V_f, indicating that this last method is more useful when describing individual maximum overtopping events, whereas V_f is mostly representative of average conditions. Mean V_f volumes are of the same order of magnitude as the individual discharges recorded in Pullen *et al.* (2003), at the Samphire Hoe (about 300 l/s to 500 l/s) and the individual maximum discharges estimated by Hughes *et al.* (2012), in laboratory. However, Qarmour exceeds the mean overtopping discharges obtained at Zeebrugge by Geeraerts and Boone (2004), Q < 0.86 l/s/m for Hmo = 3.9 m and Tp = 8.6 s, and Qarmour and Qcrest exceed the mean overtopping discharges obtained at Ostia, Q < 0.36 l/s/m for Hmo = 2.0 m and Tp = 9 s by De Rouck *et al.* (2005), as can be seen in Table 3. The differences are due to the intrinsic differences between the structures, the wave conditions and, of course, also the type of data acquisition and methodology adopted for discharge computation.

Calculated *vs.* predicted overtopping

Maximum mean overtopping discharges predicted with the EurOtop formulae were 1.2 l/s/m and 1.5x10^{-1} l/s/m at the top of the armour slope and at the beginning of the impermeable crest, respectively (Table 3). For the NN_OVERTOPPING2 tool, maximum mean overtopping discharges corrected to account for
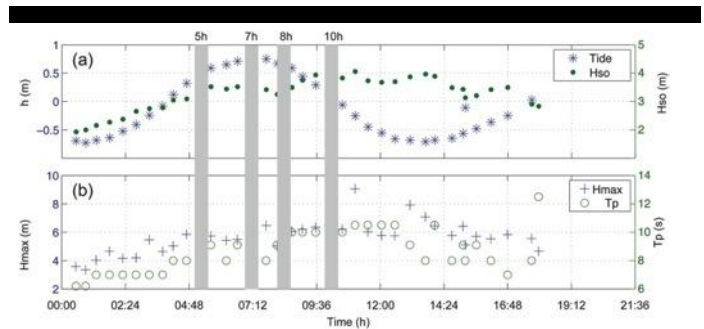

Figure 3. (a) Tide (h) and significant wave height (Hso) during fieldwork; (b) Maximum wave height (Hmax) and wave peak period (Tp) during fieldwork. Vertical grey bars mark 05h, 07h, 08h and 10h time blocks chosen for analysis of overtopping.

model, scale and wind effects in prototype situations, Q'_NN, were 1.8 l/s/m at the top of the armour slope and 5.5x10^{-1} l/s/m at the beginning of the impermeable crest. Q'_NN and Q_NN exhibit a similar pattern (Figure 5).

NN_OVERTOPPING2 mean discharges presented relatively small variations along the studied period, while the calculated mean discharges based on field measurements revealed higher variability (Figure 5, left panel). At both locations (armour and crest), Q'_NN predicted discharges present a good agreement with the calculated discharges (Qarmour and Qcrest), when considering the entire period of analysis, and are generally included in the 95% confidence intervals obtained from the NN_OVERTOPPING2 tool. Differences can be found when comparing each time block individually. At the top of the armour slope, the mean relative error between Qarmour and Q'_NN is less than 1%, whereas the maximum relative error is of 60%. At the beginning of the impermeable crest, the mean relative error between Qcrest and Q'_NN is higher, about 20%, whereas the maximum relative error is similar, 60%. The correction applied by this tool improves significantly the agreement between predicted and calculated
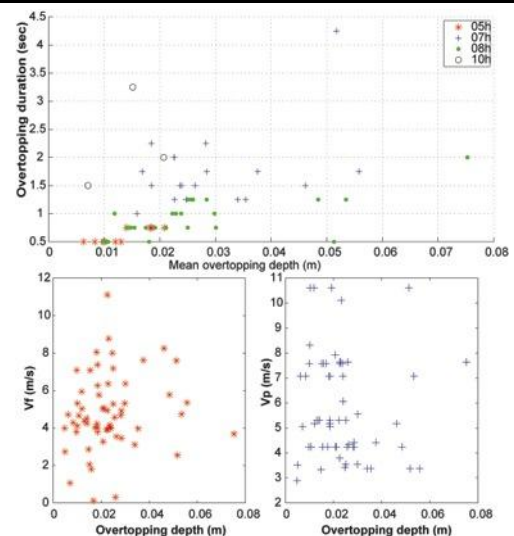

Figure 4. Overtopping duration *vs.* mean overtopping depth (upper panel); v_f and v_p vs. mean overtopping depth at the top of the breakwater armour slope (lower panel).

Table 2. V_f and V_{max} (l/m) at the beginning of the impermeable crest of the breakwater.

Parameters	V_f			
	05h	07h	08h	10h
Mean	166	170	185	181
Max	166	209	231	205
	V_{max}			
Mean	166	188	308	204
Max	166	297	508	261

Table 3. Results of mean overtopping discharges based on field measurements (Qarmour and Qcrest) and on predictions from NN_OVERTOPPING2 and EurOtop formulae (l/s/m).

	Q_{armour}	Q_NN	Q_NN (2.5%)	Q_NN (97.5%)	Q'_NN
Min	3.5×10^{-01}	2.1×10^{-01}	3.5×10^{-02}	1.3	5.5×10^{-01}
Max	2.1	1.5	2.7×10^{-01}	6.6	1.8
	Q_{crest}	Q_NN	Q_NN (2.5%)	Q_NN (97.5%)	Q'_NN
Min	1.8×10^{-01}	3.0×10^{-02}	5.4×10^{-03}	1.5×10^{-01}	1.9×10^{-01}
Max	7.5×10^{-01}	2.2×10^{-01}	6.6×10^{-02}	7.9×10^{-01}	5.5×10^{-01}
EurOtop formulae					
	Q_{armour}		Q_{crest}		
Min	1.9×10^{-01}		1.7×10^{-02}		
Max	1.2		1.5×10^{-01}		

discharges (Figure 5).

There is a fair agreement between Q'_NN and Qarmour, with three of the four data points included in-between $1/2 < Q'\_NN/Qarmour < 2$ (Figure 5, right panel). At the beginning of the impermeable crest, calculated mean overtopping discharges are also fairly predicted by NN_OVERTOPPING2 tool. In contrast, the probabilistic EurOtop formulae clearly underpredict the discharges at both locations, but especially at the impermeable crest, by one order of magnitude (Figure 5, right panel). Similar situation occurs for the uncorrected NN_OVERTOPPING2 results (Figure 5, left panel).

Deviations between fieldwork data and tools predictions can be partially explained by the natural wave variability, namely wave-wave interaction near the structure (specifically due to reflected waves) and also by the important 3D processes that occur at the field including the longshore variability of the overwash progression through structure, induced by alongshore differences between wave crest and structure. Furthermore, the calculation of overtopping discharges from field measurements use tide levels and wave conditions at the structure predicted from measurements elsewhere, which might introduce some uncertainty. Moreover, most data used for developing the tools were obtained from physical model tests, where some scale effects affect the results and where 3D effects are often neglected. The 95% confidence interval obtained from the NN_OVERTOPPING2 tool already accounts for differences on wave characteristics at the toe of the structure (before or after breaking, for example) and differences

on the measurements due to scale effects. Other deviations between fieldwork data and tools predictions can also be explained by difficulties inherent to the field measurements.

Summing up, results from the corrected NN_OVERTOPPING2 (Q'_NN) are the best predictions for mean overtopping discharges calculated based on field measurements of flow depths and velocities (Figure 5).

Hazard assessment

Because in almost all instances, the use of empirical methods involves some degree of simplification of the actual situation, the hazard analysis of the monitored conditions is discussed based on the recorded field data only.

For the calculated mean overtopping discharges $(0.2 < Qcrest < 0.8 \text{ l/s/m})$, the breakwater offers risk mostly to unaware and aware pedestrians $(Q > 0.1 \text{ l/s/m}, \text{Table 1})$. However, for the calculated overtopping peak volumes $(166 < V_{max} < 508 \text{ l/m})$, the breakwater offers risk to all types of pedestrians $(V_{max} > 500 \text{ l/m}, \text{Table 1})$, confirming visual observations during fieldwork and video monitoring. There was no related risk to small boat in the fishing harbour, since they were more than 20 m
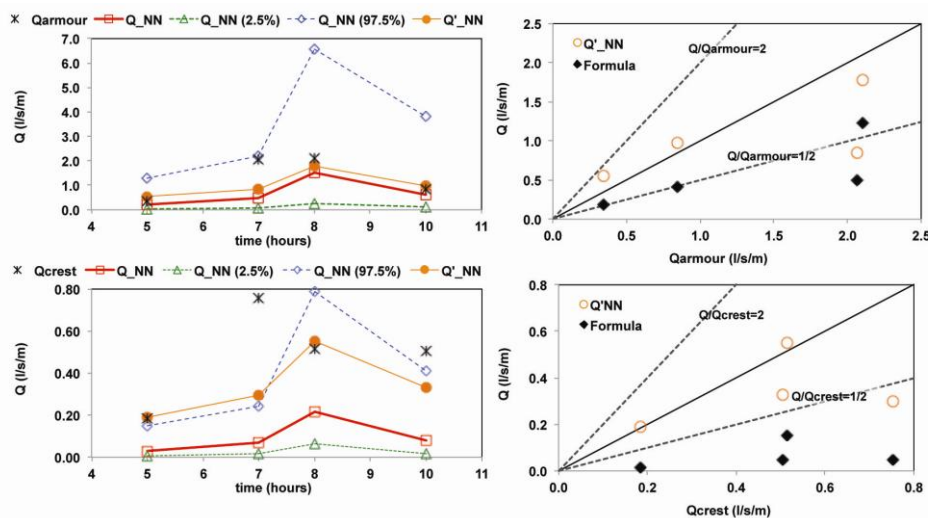

Figure 5. Comparison between calculated mean overtopping discharges based on field measurements at the top of the armour slope (Qarmour, upper panel) and at the beginning of the impermeable crest (Qcrest, lower panel), and NN_OVERTOPPING2 tool parameters (Q_NN, 95% confidence intervals, Q_NN(2.5%), Q_NN(97.5%)) (left panel); and comparison between calculated mean overtopping discharges and results from both EurOtop formulae and the NN_OVERTOPPING2 tool Q'_NN (right panel).

apart from the structure. There is a limitation when comparing the recorded hydrodynamic conditions with the classification from Table 1 since discharge intervals presented in Table 1 concern hazard assessment behind the breakwater, and the discharges presented here are related to measurements at the beginning of the impermeable crest, which seems more adequate to pedestrians at the walkway. Moreover, limits presented in Table 1 concern to overtopping velocities below 10 m/s (Allsop *et al.,* 2008). Individual maximum velocities recorded here were above 10 m/s (Figure 4), therefore, lower volume intervals should be preferably used as guideline.

Differences between the calculated mean and maximum overtopping volumes (V_f and V_{max} in l/m, Table 2), confirm the randomness of the overtopping spectrum (as suggested by Allsop *et al.* (2008)). In fact, in a precautionary management approach, individual maximums would be more adequate to characterise local overtopping hazard. Tests on the effects of overtopping flows on people suggest that values on mean discharges alone may not give reliable information (Allsop *et al.*, 2008). Thus, an increased effort to develop methods to predict maximum volumes for the overall structure types, and their validation, should be performed. The methodology applied here allows the computation of both mean and maximum volume intervals. Although it was only validated for this breakwater, it is likely suitable to be adopted in other locations. Simultaneously, besides flow depths and overtopping discharges, research should also explore in more detail the overtopping hazard estimates based on overtopping velocities.

CONCLUSIONS

This paper presents a comparison of mean overtopping discharges calculated from flow field measurements of depths and velocities at a breakwater armour and crest, with mean discharges predicted by empirical tools. The corrected NN_OVERTOPPING2 is the method that better predicted the mean discharges calculated based on field data, for the overall analysed overtopping events, but presents significant errors when predicting individual mean discharges. EurOtop formula underpredicts calculated mean discharges, and is unsuitable to predict local overtopping volumes. Towards an increase of validation of the empirical/numerical tools (*e.g.*, discharge predictions for short-term intervals) efforts should be concentrated on fieldwork data acquisition.

The recorded hydrodynamic conditions offer risk to all types of pedestrians at the walkway and to small boats, if located at less than 20 m of the breakwater. Hazard assessment has different results when using calculated mean overtopping discharges or overtopping peak volumes, thus it is recommended that peak volumes should be more often used as a parameter to infer local hazard. Future work should aim at the understanding and quantification of overtopping effects, in an attempted to solve structure design problems before construction.

ACKNOWLEDGEMENTS

LITERATURE CITED

Allsop, W., Bruce, T., Pullen, T. and van Der Meer, J., 2008. Direct Hazard from wave overtopping – the forgotten aspect of coastal flood risk assessment? DEFRA. *Proceedings of Flood and Coastal Management Conference*, Manchester, UK, 11 p.

Battjes, J.A. and Janssen, P.A.E.M., 1978. Energy loss and set-up due to breaking of random waves, *Proceedings of 16th International Conference on Coastal Engineering*, ASCE, 569-587.

Booij, N., Ris, R.C. and Holthuijsen, L.H., 1999. A third-generation wave model for coastal regions, Part I, Model description and validation, *Journal of Geophysical Research*, C4, 104, 7649-7666.

Chini, N. and Stansby, P.K., 2012. Extreme values of coastal wave overtopping accounting for climate change and sea level rise, *Coastal Engineering*, 65, 27–37.

Coeveld, E.M., Van Gent, M.R.A. and Pozueta, B., 2005. Neural Network. Manual NN_OVERTOPPING 2. CLASH WP8, WL Delft Hydraulics Report, Delft, The Netherlands.

De Rouck, J., Geeraerts, J., Troch, P., Kortenhaus, A., Pullen, T. and Franco, L., 2005. New results on scale effects for wave overtopping at coastal structures. *Proceedings of ICE Coastlines, Structures & Breakwaters '05*, Thomas Telford, London, 29-43.

Didier E., Ferreira O., Matias A., Neves M.G., Reis M.T. and Pacheco A., 2011. Desenvolvimento e validação de um modelo Smoothed Particle Hydrodynamics para aplicação a estruturas costeiras. *Proceedings of 7as Jornadas Portuguesas de Engenharia Costeira e Portuária*, eds. Delegação Portuguesa da PIANC, pp 30 (15 p. CD Rom), Porto, Portugal.

Ferreira, Ó., Reis, M.T., Carrasco, A.R., Neves, M.G., and Didier, E., 2013. Small Overtopping discharges at Albufeira Harbour: field measurements and modelling. *Proceedings of 6th SCACR – International Short Course/Conference on Applied Coastal Research*, LNEC, Lisboa.

Geeraerts, J. and Boone, C., 2004. CLASH: Full Scale Measurements on the Zeebrugge breakwater - Second Winter Season, Ghent University, Belgium.

Geeraerts, J., Troch, P., Rouck, J.D., Verhaeghe, H. and Bouma, J.J., 2007. Wave overtopping at coastal structures: prediction tools and related hazard analysis. *Journal of Clear Production*, 15, 1514-1521.

Hasselmann, K., Barnett, T.P., Bouws, E., Carlson, H., Cartwright, H., Cartwright, D.E., Enke, K., Ewing, J.A., Gienapp, H., Hasselmann, D.E.,Kruseman, P., Meerburg, A., Muller, P., Olbers, D.J., Richter, K., Sell, W. and Walden, H., 1973. Measurements of wind-wave growth and swell decay during the Joint North Sea Wave Project (JONSWAP). Dtsch. Hydrogr. Z. Suppl. 12 (A8), 1–95.

Holthuijsen, L.H., 2007. Waves in Oceanic and Coastal Waters, Cambridge University Press.

Hughes, S., Thornton, C., van der Meer, J. and Scholl, B., 2012. Improvements in describing wave overtopping processes. *Proceedings of 3rd International Conference Coastal Engineering (ICCE)*, ASCE, Santander, Spain, 1-6.

Pullen, T., Allsop, N.W.H., Bruce, T. and Geeraerts, J., 2003. Violent wave overtopping: CLASH field measurements at Samphire Hoe. *Proceeding of Coastal Structures*, 12 p.

Pullen, T., Allsop, N.W.H., Bruce, T., Kortenhaus, A., Schü☐ttrumpf, H. And Van der Meer, J.W., 2007. EurOtop: Wave Overtopping of Sea Defences and Related Structures: Assessment Manual. Environment Agency, UK, Expertise Netwerk Waterkeren, NL, and Kuratorium fur Forschung im Kusteningenieurwesen, DE.

Shankar, N.J. and Jayaratne, M.P.R., 2003. Wave run-up and overtopping on smooth and rough slopes of coastal structures. *Ocean Engineering*, 30, 221-238.

Tonelli, M. and Petti, M., 2013. Numerical simulation of wave overtopping at coastal dikes and low crested structures by means of a shock-capturing Boussinesq model. *Coastal Engineering*, 79, 75–88.

Van der Meer, J.W., Snijders, W., and Regeling, H.J. 2006. The wave overtopping simulator. *Proceedings of 30th International Conference Coastal Engineering*, ASCE, San Diego, 4654-4679.

Verhaeghe, H., 2005. Neural Network Prediction of Wave Overtopping at Coastal Structures. PhD Thesis, Gent University, Belgium.